Mathematics

http://www.aimspress.com/journal/Math

AIMS Mathematics, 11(8): 27563–27584.
DOI: 10.3934/math.20261103
Received: 26 May 2026
Revised: 07 August 2026
Accepted: 24 August 2026
Published: 31 August 2026

Research article

Optimal H^1-norm error analysis of an IMEX BDF2 nonconforming virtual element scheme for the Allen-Cahn equation

Peizhen Wang*, **Wang Liu and Jinyang Xia**

School of Mathematics and Statistics, North China University of Water Resources and Electric Power, Zhengzhou 450046, China

* **Correspondence:** Email: peizhen86@126.com.

Abstract: We developed a fully discrete scheme for the Allen-Cahn equation on polygonal meshes by combining a second-order implicit-explicit (IMEX) backward differentiation formula (BDF2) with a nonconforming virtual element method for spatial discretization. To rigorously justify the global Lipschitz condition required in the analysis, we employed an explicitly defined truncated polynomial potential that coincided with the standard quartic double-well potential on $[-M, M]$ and had quadratic growth outside this interval. Under a suitable time-step restriction, the proposed scheme satisfied a modified discrete energy dissipation law. Optimal error estimates of order $O(h^{k+1} + \tau^2)$ in the L^2-norm and $O(h^k + \tau^2)$ in the H^1-seminorm were established. In particular, a discrete Laplace operator adapted to the nonconforming virtual element space was introduced to avoid temporal order reduction in the H^1-error analysis. Numerical experiments confirmed the theoretical convergence rates.

Keywords: Allen-Cahn equation; nonconforming virtual element method; IMEX BDF2; modified energy stability; optimal H^1-norm error estimate
Mathematics Subject Classification: 65M06, 65M12

1. Introduction

The Allen-Cahn model, originally proposed by Allen and Cahn [1], is a fundamental phase-field equation for describing antiphase-boundary motion and interfacial dynamics in crystalline materials. We consider the following two-dimensional Allen-Cahn problem:

$$\begin{cases} u_t - \varepsilon\Delta u + \widetilde{f}(u) = 0, & (x,t) \in \Omega \times (0,T], \\ u = 0, & (x,t) \in \partial\Omega \times (0,T], \\ u(x,0) = u^0(x), & x \in \Omega, \end{cases} \tag{1.1}$$

where $\Omega \subset \mathbb{R}^2$ is a bounded convex polygonal domain, $\varepsilon > 0$ denotes the interfacial-width parameter, and u represents the phase variable.

The standard quartic double-well potential

$$F_{\mathrm{dw}}(s) = \frac{1}{4}(s^2 - 1)^2$$

gives the cubic nonlinear function

$$f_{\mathrm{dw}}(s) = s^3 - s.$$

However,

$$f'_{\mathrm{dw}}(s) = 3s^2 - 1$$

is unbounded on $\mathbb{R}$ and therefore does not satisfy the global Lipschitz condition required in the stability and error analyses.

Following Shen and Yang [2], for a fixed truncation threshold $M \geq 1$, we replace the quartic potential by the quadratic-growth truncated potential

$$\widetilde{F}(s) = \begin{cases} \dfrac{3M^2 - 1}{2}s^2 - 2M^3 s + \dfrac{1}{4}(3M^4 + 1), & s > M, \\ \dfrac{1}{4}(s^2 - 1)^2, & |s| \leq M, \\ \dfrac{3M^2 - 1}{2}s^2 + 2M^3 s + \dfrac{1}{4}(3M^4 + 1), & s < -M. \end{cases} \tag{1.2}$$

Its derivative is

$$\widetilde{f}(s) = (\widetilde{F})'(s) = \begin{cases} (3M^2 - 1)s - 2M^3, & s > M, \\ s^3 - s, & |s| \leq M, \\ (3M^2 - 1)s + 2M^3, & s < -M. \end{cases} \tag{1.3}$$

The values and the first two derivatives of $\widetilde{F}$ match at $s = \pm M$. Consequently,

$$\widetilde{F} \in C^2(\mathbb{R}), \qquad \widetilde{f} \in C^1(\mathbb{R}).$$

Moreover,

$$(\widetilde{f})'(s) = \begin{cases} 3M^2 - 1, & |s| > M, \\ 3s^2 - 1, & |s| < M, \\ 3M^2 - 1, & s = \pm M. \end{cases} \tag{1.4}$$

It follows that

$$\|(\widetilde{f})'\|_{L^\infty(\mathbb{R})} = 3M^2 - 1. \tag{1.5}$$

Therefore,

$$|\widetilde{f}(r) - \widetilde{f}(s)| \leq L|r - s|, \qquad r, s \in \mathbb{R}, \qquad L = 3M^2 - 1. \tag{1.6}$$

The truncated potential agrees exactly with the standard quartic double-well potential on $[-M, M]$. Therefore, if the exact solution satisfies

$$\|u\|_{L^\infty(0,T;L^\infty(\Omega))} \leq M,$$

the original and truncated Allen-Cahn equations coincide along the exact solution.

The corresponding energy functional is

$$E(u) = \int_{\Omega} \left(\frac{\varepsilon}{2} |\nabla u|^2 + \widetilde{F}(u) \right) dx. \tag{1.7}$$

For a sufficiently regular solution, testing (1.1) by u_t gives

$$\frac{d}{dt} E(u(t)) = -\|u_t(t)\|_0^2 \leq 0.$$

The variational formulation of (1.1) is to find $u \in L^2(0, T; H_0^1(\Omega))$ such that

$$\begin{cases} m(u_t, v) + \varepsilon a(u, v) + (f(u), v) = 0, \ \forall v \in H_0^1(\Omega), \\ u(0) = u^0, \end{cases} \tag{1.8}$$

where

$$m(u, v) = \int_{\Omega} uv \, dx, \quad a(u, v) = \int_{\Omega} \nabla u \cdot \nabla v \, dx.$$

Since analytical solutions are generally unavailable, efficient and stable numerical methods are of considerable importance. Various approaches have been developed for the Allen-Cahn equation. Finite difference methods were studied in [3–5] for mimetic operators, explicit stability, and discrete maximum principles, and in [6] for exponential time differencing schemes. Finite element methods were investigated in [7–9] for stabilized formulations, maximum-principle-preserving schemes, and the backward differentiation formula (BDF) error analyses. Weak Galerkin methods were developed in [10, 11] with scalar auxiliary variable and a second-order backward differentiation formula (BDF2) approaches. Discontinuous Galerkin methods were considered in [12] on polygonal meshes.

The virtual element method (VEM), introduced in [13], provides considerable flexibility on general polygonal meshes. It avoids the explicit construction of virtual basis functions and permits the use of polygonal elements with complex shapes. The VEM has been applied to various problems. Parabolic equations were studied in [14] and elasticity problems in [15]. The Stokes and Navier-Stokes equations were addressed in [16], while Maxwell equations were treated in [17]. Allen-Cahn-type gradient flows [18] and the Cahn-Hilliard equation [19] have also been investigated within the VEM framework.

The theoretical distinction between conforming and nonconforming VEM is crucial to our analysis. In the conforming case,$V_h \subset H_0^1(\Omega)$ permits direct use of C*é*a's lemma and Galerkin orthogonality. For nonconforming VEM, $V_h \not\subset H_0^1(\Omega)$, so gradients are only elementwise defined and interelement jumps cannot be neglected. This gives rise to two major challenges: (i) The error analysis invokes the second Strang lemma, requiring careful control of consistency errors via weak continuity (edge/face moments); (ii) A discrete broken H^1-seminorm is needed, and crucially, a modified discrete Laplace operator Δ_h must be constructed to close the test procedure for optimal H^1-error estimates under BDF2 without order reduction. These nonconforming-specific difficulties make our optimal error estimate for the Allen-Cahn equation theoretically nontrivial and methodologically significant.

Analogous to nonconforming finite element methods, the nonconforming VEM relaxes the interelement continuity requirements. The nonconforming VEM was introduced in [20]. It was subsequently extended to the Stokes equations in [21], the Navier-Stokes equations in [22], and the divergence-free formulation for Navier-Stokes in [23]. The Darcy-Stokes problem was considered in [24], coupled Ginzburg-Landau equations in [25], plate-bending problems in [26], linear elasticity in [27], and the Cahn-Hilliard equation in [28].

To the best of our knowledge, the optimal broken-H^1 error analysis of an implicit-explicit (IMEX) BDF2 nonconforming VEM for the Allen-Cahn equation has not yet been established.

The proposed method has several advantages. First, the VEM permits general polygonal meshes and therefore offers considerable geometric flexibility. Second, the nonconforming formulation relaxes global continuity requirements and uses computable edge and element moments as degrees of freedom. Third, the IMEX BDF2 discretization treats the diffusion term implicitly and the nonlinear term explicitly, so that only a linear algebraic system is solved at each time level. Finally, the discrete Laplace operator introduced in this work leads to an optimal second-order temporal estimate in the H^1-seminorm.

The method also has several limitations. Its modified energy stability is conditional and requires a sufficiently small time step. The theoretical analysis uses the truncated polynomial potential (1.2), assumes sufficient regularity of the exact solution, and is currently restricted to constant time steps and two-dimensional polygonal meshes. Moreover, no discrete maximum principle is established. Unlike (scalar auxiliary variable)- and (invariant energy quadratization)-type formulations, which can often provide unconditional stability with respect to an associated modified energy, the present method emphasizes a simple linear IMEX implementation and optimal nonconforming VEM error estimates.

The remainder of the paper is organized as follows. Section 2 introduces the nonconforming virtual element space and the discrete bilinear forms. Section 3 presents the fully discrete IMEX BDF2 scheme. Section 4 establishes the conditional dissipation of a modified discrete energy. Section 5 derives optimal L^2-norm and H^1-seminorm error estimates. Section 6 presents numerical experiments. Finally, Section 7 summarizes the principal conclusions and discusses possible extensions.

2. Nonconforming virtual element space

Let $\mathcal{T}_h$ be a family of polygonal decompositions of Ω. For each $K \in \mathcal{T}_h$, let $h_K = \mathrm{diam}(K), h = \max_{K\in\mathcal{T}_h} h_K$. Let $\mathcal{E}_h$ denote the set of all edges of the mesh.

Let K^+ and K^- be two neighboring elements sharing an interior edge e, and let $\boldsymbol{n}_e$ be the unit normal directed from K^+ to K^-. For a piecewise regular function v, its jump across e is defined by

$$[v] = v|_{K^+} - v|_{K^-} .$$

On a boundary edge $e \subset \partial\Omega$, we set $[v] = v|_e$.

For $k \geq 1$, let $\mathbb{P}_k(K)$ denote the space of polynomials of degree at most k on K. The augmented local virtual element space (see [29]) is

$$\widetilde{V}(K) = \left\{ v \in H^1(K) : \frac{\partial v}{\partial \boldsymbol{n}_e} \in \mathbb{P}_{k-1}(e),\ \forall e \subset \partial K, \quad \Delta v \in \mathbb{P}_k(K) \right\}.$$

The set of local degrees of freedom (D) consists of:

- The edge moments
$$\frac{1}{|e|}\int_e vq\,ds, \qquad q \in \mathbb{P}_{k-1}(e), \quad e \subset \partial K;$$
- The element moments
$$\frac{1}{|K|}\int_K vq\,dx, \qquad q \in \mathbb{P}_{k-2}(K).$$

Let $a^K(\cdot,\cdot)$ denote the restriction of $a(\cdot,\cdot)$ to K. The elliptic projection
$$\Pi_K^\nabla : \widetilde{V}(K) \longrightarrow \mathbb{P}_k(K)$$
is defined by
$$a^K(\Pi_K^\nabla v, q) = a^K(v, q), \qquad q \in \mathbb{P}_k(K),$$
together with
$$\int_{\partial K} \Pi_K^\nabla v\,ds = \int_{\partial K} v\,ds.$$

The local virtual element space is defined by
$$V(K) = \left\{ v \in \widetilde{V}(K) : (v,q)_K = (\Pi_K^\nabla v, q)_K, \quad q \in \mathbb{P}_k(K)/\mathbb{P}_{k-2}(K) \right\}.$$

The linear functionals collected in (D) constitute a unisolvent set of degrees of freedom for the local virtual element space $V(K)$. Here, $\mathbb{P}_k(K)/\mathbb{P}_{k-2}(K)$ is understood as the $L^2(K)$-orthogonal complement of $\mathbb{P}_{k-2}(K)$ in $\mathbb{P}_k(K)$. These degrees of freedom permit the polynomial projections Π_K^∇ and Π_K^0 to be computed without explicitly constructing the virtual basis functions.

The global nonconforming virtual element space is
$$V_h = \left\{ v \in L^2(\Omega) : v|_K \in V(K),\ \forall K \in \mathcal{T}_h, \quad \int_e [v] q\,ds = 0\ \forall q \in \mathbb{P}_{k-1}(e),\ \forall e \in \mathcal{E}_h \right\}.$$

Since $V_h \not\subset H_0^1(\Omega)$, we use the discrete seminorm
$$|v|_{1,h} = \left(\sum_{K\in\mathcal{T}_h} |v|_{1,K}^2 \right)^{1/2}.$$

For each $K \in \mathcal{T}_h$, define
$$a_h^K(v,w) = a^K(\Pi_K^\nabla v, \Pi_K^\nabla w) + S^K((I-\Pi_K^\nabla)v, (I-\Pi_K^\nabla)w)$$
and
$$m_h^K(v,w) = (\Pi_K^0 v, \Pi_K^0 w)_K + |K| S^K((I-\Pi_K^0)v, (I-\Pi_K^0)w).$$

We choose a symmetric positive definite stabilization $S^K(\cdot,\cdot)$ of the form
$$S^K(v,w) = \sum_{j=1}^{N^K} X_j(v) X_j(w), \quad N^K = \dim V(K),$$

where $X_j(v)$ denotes the jth scaled degree of freedom of v on K.

The discrete bilinear forms satisfy the polynomial consistency properties

$$a_h^K(v,p) = a^K(v,p), \quad m_h^K(v,p) = (v,p)_K,$$

for all $v \in V(K)$ and $p \in \mathbb{P}_k(K)$.

Moreover, there exist positive constants $\alpha_*, \alpha^*, \beta_*, \beta^*$, independent of h, such that

$$\alpha_* a^K(v,v) \le a_h^K(v,v) \le \alpha^* a^K(v,v)$$

and

$$\beta_* \|v\|_{0,K}^2 \le m_h^K(v,v) \le \beta^* \|v\|_{0,K}^2.$$

The global discrete bilinear forms are

$$a_h(v,w) = \sum_{K\in\mathcal{T}_h} a_h^K(v,w), \quad m_h(v,w) = \sum_{K\in\mathcal{T}_h} m_h^K(v,w).$$

Consequently,

$$|a_h(v,w)| \le \alpha^* |v|_{1,h} |w|_{1,h}$$

and

$$|m_h(v,w)| \le \beta^* \|v\|_0 \|w\|_0.$$

Lemma 2.1. *([30]) Let P^h: $H^{k+1}(\Omega)\cap H_0^1(\Omega) \longrightarrow V_h$ be the energy projection defined by*

$$a_h(P^h u, v_h) = (-\Delta u, v_h), \quad \forall v_h \in V_h.$$

Then, for every $u \in H^{k+1}(\Omega)\cap H_0^1(\Omega)$,

$$|u - P^h u|_{1,h} \le C h^k |u|_{k+1} \tag{2.1}$$

and

$$\|u - P^h u\|_0 \le C h^{k+1} |u|_{k+1}. \tag{2.2}$$

Here and below, $C > 0$ denotes a generic constant independent of h and τ, although it may depend on the domain, mesh regularity, ε, T, and appropriate norms of the exact solution.

3. Fully discrete scheme

Let

$$0 = t_0 < t_1 < \cdots < t_N = T, \quad t_n = n\tau, \quad \tau = \frac{T}{N}.$$

We write

$$u^n = u(\cdot, t_n)$$

and denote the fully discrete solution at t_n by $u_h^n \in V_h$.

For $v_h \in V_h$, define the discrete nonlinear function elementwise by

$$\widetilde{f}_h(v_h)\Big|_K = \Pi_K^0\left(\widetilde{f}(\Pi_K^0 v_h)\right), \quad K \in \mathcal{T}_h. \tag{3.1}$$

The fully discrete IMEX BDF2 (see [31]) nonconforming VEM scheme is to find $u_h^{n+1} \in V_h$, for $n \geq 1$, such that

$$\begin{cases} m_h\left(\dfrac{3u_h^{n+1} - 4u_h^n + u_h^{n-1}}{2\tau}, v_h\right) + \varepsilon a_h(u_h^{n+1}, v_h) + \left(2\widetilde{f}_h(u_h^n) - \widetilde{f}_h(u_h^{n-1}), v_h\right) = 0, \qquad \forall v_h \in V_h, \\ u_h^0 = P^h u^0. \end{cases} \tag{3.2}$$

The first value u_h^1 is computed using the first-order backward differentiation formula (BDF1) initialization described in Remark 5.1.

Lemma 3.1. *([25]) Assume that*

$$u_{ttt} \in L^\infty(0, T; L^2(\Omega)).$$

Then,

$$\left\| u_t^{n+1} - \frac{3u^{n+1} - 4u^n + u^{n-1}}{2\tau} \right\|_0 \leq C\tau^2 \|u_{ttt}\|_{L^\infty(0,T;L^2(\Omega))}. \tag{3.3}$$

4. Conditional modified energy stability

For $v_h \in V_h$, define the discrete potential energy by

$$\mathcal{F}_h(v_h) = \sum_{K \in \mathcal{T}_h} \int_K \widetilde{F}(\Pi_K^0 v_h)\, dx, \tag{4.1}$$

and the discrete physical energy by

$$E_h(v_h) = \frac{\varepsilon}{2} a_h(v_h, v_h) + \mathcal{F}_h(v_h). \tag{4.2}$$

Define the discrete mass norm by

$$\|v_h\|_{m_h}^2 = m_h(v_h, v_h).$$

The stability of m_h gives

$$\beta_* \|v_h\|_0^2 \leq \|v_h\|_{m_h}^2 \leq \beta^* \|v_h\|_0^2. \tag{4.3}$$

For $n \geq 1$, let

$$d_h^{n+1} = u_h^{n+1} - u_h^n.$$

The modified discrete energy is defined by

$$\mathcal{H}_h^{n+1} = E_h(u_h^{n+1}) + \eta_\tau \left\| d_h^{n+1} \right\|_{m_h}^2, \quad \eta_\tau = \frac{1}{4\tau} + \frac{L}{2\beta_*}, \tag{4.4}$$

where $L = 3M^2 - 1$.

Theorem 4.1. *If*

$$\tau \leq \frac{2\beta_*}{3L}, \tag{4.5}$$

then the solution of (3.2) *satisfies*

$$\mathcal{H}_h^{n+1} \leq \mathcal{H}_h^n, \quad n \geq 1. \tag{4.6}$$

Thus, the proposed IMEX BDF2 scheme is conditionally stable with respect to the modified discrete energy (4.4).

Proof. Taking

$$v_h = d_h^{n+1}$$

in Eq (3.2) gives

$$m_h\left(\frac{3d_h^{n+1} - d_h^n}{2\tau}, d_h^{n+1}\right) + \varepsilon a_h(u_h^{n+1}, d_h^{n+1}) + \left(2\widetilde{f}_h(u_h^n) - \widetilde{f}_h(u_h^{n-1}), d_h^{n+1}\right) = 0. \tag{4.7}$$

The symmetry of a_h gives

$$a_h(u_h^{n+1}, d_h^{n+1}) = \frac{1}{2}[a_h(u_h^{n+1}, u_h^{n+1}) - a_h(u_h^n, u_h^n) + a_h(d_h^{n+1}, d_h^{n+1})]. \tag{4.8}$$

By Taylor's theorem and $\|(\widetilde{f})'\|_{L^\infty(\mathbb{R})} \leq L$,

$$\mathcal{F}_h(u_h^{n+1}) - \mathcal{F}_h(u_h^n) \leq \left(\widetilde{f}_h(u_h^n), d_h^{n+1}\right) + \frac{L}{2}\|\Pi^0 d_h^{n+1}\|_0^2. \tag{4.9}$$

The global Lipschitz continuity of $\widetilde{f}$ yields

$$\left|\left(\widetilde{f}_h(u_h^n) - \widetilde{f}_h(u_h^{n-1}), d_h^{n+1}\right)\right| \leq L\|\Pi^0 d_h^n\|_0\|\Pi^0 d_h^{n+1}\|_0 \leq \frac{L}{2}\left(\|d_h^n\|_0^2 + \|d_h^{n+1}\|_0^2\right). \tag{4.10}$$

For the BDF2 term, the Cauchy-Schwarz and Young inequalities in the m_h inner product give

$$m_h\left(\frac{3d_h^{n+1} - d_h^n}{2\tau}, d_h^{n+1}\right) \geq \frac{5}{4\tau}\left\|d_h^{n+1}\right\|_{m_h}^2 - \frac{1}{4\tau}\left\|d_h^n\right\|_{m_h}^2. \tag{4.11}$$

Combining (4.7)–(4.11) and using (4.3), we obtain

$$\begin{aligned}
&E_h(u_h^{n+1}) - E_h(u_h^n) + \frac{\varepsilon}{2}a_h(d_h^{n+1}, d_h^{n+1}) + \left(\frac{5}{4\tau} - \frac{L}{\beta_*}\right)\left\|d_h^{n+1}\right\|_{m_h}^2 \\
&= \frac{\varepsilon}{2}a_h(u_h^{n+1}, u_h^{n+1}) - \frac{\varepsilon}{2}a_h(u_h^n, u_h^n) + \mathcal{F}_h(u_h^{n+1}) - \mathcal{F}_h(u_h^n) + \frac{\varepsilon}{2}a_h(d_h^{n+1}, d_h^{n+1}) + \left(\frac{5}{4\tau} - \frac{L}{\beta_*}\right)\left\|d_h^{n+1}\right\|_{m_h}^2 \\
&\leq \varepsilon a_h(u_h^{n+1}, d_h^{n+1}) + \left(f_h^{tr}(u_h^n), d_h^{n+1}\right) + \frac{L}{2}\|\Pi^0 d_h^{n+1}\|_0^2 + \left(\frac{5}{4\tau} - \frac{L}{\beta_*}\right)\left\|d_h^{n+1}\right\|_{m_h}^2 \\
&= -m_h\left(\frac{3d_h^{n+1} - d_h^n}{2\tau}, d_h^{n+1}\right) - \left(f_h^{tr}(u_h^n) - f_h^{tr}(u_h^{n-1}), d_h^{n+1}\right) + \frac{L}{2}\|\Pi^0 d_h^{n+1}\|_0^2 + \left(\frac{5}{4\tau} - \frac{L}{\beta_*}\right)\left\|d_h^{n+1}\right\|_{m_h}^2 \\
&\leq \frac{1}{4\tau}\left\|d_h^n\right\|_{m_h}^2 - \frac{5}{4\tau}\left\|d_h^{n+1}\right\|_{m_h}^2 + \frac{L}{2\beta_*}\left(\left\|d_h^{n+1}\right\|_{m_h}^2 + \left\|d_h^n\right\|_{m_h}^2\right) + \frac{L}{2\beta_*}\left\|d_h^{n+1}\right\|_{m_h}^2 + \left(\frac{5}{4\tau} - \frac{L}{\beta_*}\right)\left\|d_h^{n+1}\right\|_{m_h}^2 \\
&= \left(\frac{1}{4\tau} + \frac{L}{2\beta_*}\right)\left\|d_h^n\right\|_{m_h}^2.
\end{aligned} \tag{4.12}$$

Condition (4.5) implies

$$\frac{5}{4\tau} - \frac{L}{\beta_*} \geq \frac{1}{4\tau} + \frac{L}{2\beta_*} = \eta_\tau.$$

Dropping the nonnegative diffusion-increment term gives

$$E_h(u_h^{n+1}) + \eta_\tau\left\|d_h^{n+1}\right\|_{m_h}^2 \leq E_h(u_h^n) + \eta_\tau\left\|d_h^n\right\|_{m_h}^2.$$

This is exactly (4.6). □

Remark 4.1. *The stability result concerns the modified energy $\mathcal{H}_h^n$, which differs from the physical energy $E_h(u_h^n)$ by a consistent BDF2 increment term. Such modified energies are commonly used in the stability analysis of higher-order multistep schemes. The stability is conditional because* (4.5) *imposes an upper bound on the time-step size.*

5. Error estimates

5.1. Error estimate in the L^2-norm

We assume that

$$\begin{aligned} u \in L^\infty(0,T;H^{k+1}(\Omega)),\ \ u_t \in L^\infty(0,T;H^{k+1}(\Omega)),\\ u_{ttt} \in L^\infty(0,T;L^2(\Omega)),\ \ \widetilde{f} \in L^\infty(0,T;H^{k+1}(\Omega)) \cap W^{2,\infty}(0,T;L^2(\Omega)). \end{aligned} \tag{5.1}$$

Define

$$\begin{aligned} \mathcal{R}_{h,\tau} = Ch^{k+1}\Big(\|u\|_{L^\infty(0,T;H^{k+1}(\Omega))} + \|u_t\|_{L^\infty(0,T;H^{k+1}(\Omega))} + \|\widetilde{f}\|_{L^\infty(0,T;H^{k+1}(\Omega))}\Big)\\ + C\tau^2\Big(\|u_{ttt}\|_{L^\infty(0,T;L^2(\Omega))} + \|\widetilde{f}_{tt}\|_{L^\infty(0,T;L^2(\Omega))}\Big). \end{aligned} \tag{5.2}$$

Theorem 5.1. *Let $u^{n+1} = u(\cdot, t_{n+1})$ be the exact solution of* (1.8)*, and let u_h^{n+1} be the solution of* (3.2)*. Under* (5.1)*, and for sufficiently small τ, there exists a constant $C > 0$, independent of h and τ, such that*

$$\|u_h^{n+1} - u^{n+1}\|_0 \le C\left(\|u_h^1 - u^1\|_0 + \mathcal{R}_{h,\tau}\right). \tag{5.3}$$

Proof. We set

$$u_h^{n+1} - u^{n+1} = (u_h^{n+1} - P^h u^{n+1}) + (P^h u^{n+1} - u^{n+1}) \triangleq A^{n+1} + B^{n+1}. \tag{5.4}$$

Utilizing (2.2), we obtain

$$\|B^{n+1}\|_0 \le Ch^{k+1}\|u\|_{L^\infty(0,T;H^{k+1}(\Omega))}. \tag{5.5}$$

To estimate $\|A^{n+1}\|_0$, we first undertake some preparatory work. Let

$$U^{n+1} = 3u^{n+1} - 4u^n + u^{n-1},$$

and by the compatibility of $m_h(\cdot,\cdot)$, we have

$$\begin{aligned} (u_t^{n+1}, v_h) - m_h\left(\frac{P^h U^{n+1}}{2\tau}, v_h\right) = \left(u_t^{n+1} - \frac{U^{n+1}}{2\tau}, v_h\right) + \left(\frac{U^{n+1} - \Pi_K^0 U^{n+1}}{2\tau}, v_h\right)\\ + m_h\left(\frac{\Pi_K^0 U^{n+1} - P^h U^{n+1}}{2\tau}, v_h\right). \end{aligned} \tag{5.6}$$

Based on the definition of f_h, we can obtain

$$\begin{aligned} \widetilde{f}(u^{n+1}) &= \widetilde{f}(u^{n+1}) - \widetilde{f}(\Pi_K^0 u^{n+1}) + \widetilde{f}(\Pi_K^0 u^{n+1}) - \Pi_K^0(\widetilde{f}(\Pi_K^0 u^{n+1}))\\ &\quad + \Pi_K^0(\widetilde{f}(\Pi_K^0 u^{n+1})) - \Pi_K^0(\widetilde{f}(\Pi_K^0 u_h^{n+1})) + \Pi_K^0(\widetilde{f}(\Pi_K^0 u_h^{n+1}))\\ &= [\widetilde{f}(u^{n+1}) - \widetilde{f}(\Pi_K^0 u^{n+1})] + [\widetilde{f}(\Pi_K^0 u^{n+1}) - \Pi_K^0(\widetilde{f}(\Pi_K^0 u^{n+1}))]\\ &\quad + \Pi_K^0(\widetilde{f}(\Pi_K^0 u^{n+1}) - \widetilde{f}(\Pi_K^0 u_h^{n+1})) + \widetilde{f}_h(u_h^{n+1}). \end{aligned} \tag{5.7}$$

Utilizing (1.1), (3.2), (5.6), (5.7), and the definition of U^{n+1} and P^h, we observe that

$$\begin{aligned}
&m_h\left(\frac{3A^{n+1}-4A^n+A^{n-1}}{2\tau},v_h\right)+\varepsilon a_h(A^{n+1},v_h)\\
&=\left[m_h\left(\frac{3u_h^{n+1}-4u_h^n+u_h^{n-1}}{2\tau},v_h\right)+\varepsilon a_h(u_h^{n+1},v_h)\right]\\
&\quad-\left[m_h\left(\frac{3P^hu^{n+1}-4P^hu^n+P^hu^{n-1}}{2\tau},v_h\right)+\varepsilon a_h(P^hu^{n+1},v_h)\right]\\
&=(-2\widetilde{f}_h(u_h^n)+\widetilde{f}_h(u_h^{n-1}),v_h)-m_h\left(\frac{P^hU^{n+1}}{2\tau},v_h\right)+(u_t^{n+1}+\widetilde{f}(u^{n+1}),v_h)\\
&=(\widetilde{f}(u^{n+1})-2\widetilde{f}_h(u_h^n)+\widetilde{f}_h(u_h^{n-1}),v_h)+\left[(u_t^{n+1},v_h)-m_h\left(\frac{P^hU^{n+1}}{2\tau},v_h\right)\right]\\
&=(\widetilde{f}(u^{n+1})-\widetilde{f}(\Pi_K^0u^{n+1}),v_h)+(\widetilde{f}(\Pi_K^0u^{n+1})-\Pi_K^0(\widetilde{f}(\Pi_K^0u^{n+1})),v_h)\\
&\quad+(\Pi_K^0(\widetilde{f}(\Pi_K^0u^{n+1})-\widetilde{f}(\Pi_K^0u_h^{n+1})),v_h)+(\widetilde{f}_h(u_h^{n+1})-2\widetilde{f}_h(u_h^n)+\widetilde{f}_h(u_h^{n-1}),v_h)\\
&\quad+\left(u_t^{n+1}-\frac{U^{n+1}}{2\tau},v_h\right)+\left(\frac{U^{n+1}-P^hU^{n+1}}{2\tau},v_h\right)+m_h\left(\frac{\Pi_K^0U^{n+1}-P^hU^{n+1}}{2\tau},v_h\right).\\
&\triangleq Err_1+Err_2+Err_3+Err_4+Err_5+Err_6+Err_7.
\end{aligned}\tag{5.8}$$

We now estimate the terms $Err_i(i=1,\cdots,7)$ on the righthand side one by one.

The bound for Err_1 is derived by leveraging the Lipschitz continuity of f with respect to u and the standard approximation property of the L^2 projection operator, according to [32],

$$\begin{aligned}
Err_1&=(\widetilde{f}(u^{n+1})-\widetilde{f}(\Pi_K^0u^{n+1}),v_h)\le L\|u^{n+1}-\Pi_K^0u^{n+1}\|_0\|v_h\|_0\\
&\le Ch^{k+1}\|u\|_{L^\infty(0,T;H^{k+1}(\Omega))}\|v_h\|_0.
\end{aligned}\tag{5.9}$$

Similarly,

$$Err_2=(\widetilde{f}(\Pi_K^0u^{n+1})-\Pi_K^0(\widetilde{f}(\Pi_K^0u^{n+1})),v_h)\le Ch^{k+1}\|\widetilde{f}\|_{L^\infty(0,T;H^{k+1}(\Omega))}\|v_h\|_0,\tag{5.10}$$

$$\begin{aligned}
Err_3&=(\Pi_K^0(\widetilde{f}(\Pi_K^0u^{n+1})-\widetilde{f}(\Pi_K^0u_h^{n+1})),v_h)\le\|\widetilde{f}(\Pi_K^0u^{n+1})-\widetilde{f}(\Pi_K^0u_h^{n+1})\|_0\|v_h\|_0\\
&\le L\|\Pi_K^0(u^{n+1}-u_h^{n+1})\|_0\|v_h\|_0\le L\|u^{n+1}-u_h^{n+1}\|_0\|v_h\|_0\\
&\le L(\|A^{n+1}\|_0+\|B^{n+1}\|_0)\|v_h\|_0.
\end{aligned}\tag{5.11}$$

For Err_4, by the definition of f_h, we have

$$\begin{aligned}
Err_4&=(\widetilde{f}_h(u_h^{n+1})-2\widetilde{f}_h(u_h^n)+\widetilde{f}_h(u_h^{n-1}),v_h)\\
&=(\Pi_K^0(\widetilde{f}_h(\Pi_K^0u_h^{n+1})-2\widetilde{f}_h(\Pi_K^0u_h^n)+\widetilde{f}_h(\Pi_K^0u_h^{n-1})),v_h)\\
&=\left(\Pi_K^0\left(\int_{t_n}^{t_{n+1}}\widetilde{f}_t(\cdot,t)\,dt-\int_{t_{n-1}}^{t_n}\widetilde{f}_t(\cdot,t)\,dt\right),v_h\right)\\
&=\left(\Pi_K^0\left(\int_{t_n}^{t_{n+1}}\widetilde{f}_t(\cdot,t)\,dt-\int_{t_n}^{t_{n+1}}\widetilde{f}_t(\cdot,t-\tau)\,dt\right),v_h\right)\\
&=\left(\Pi_K^0\int_{t_n}^{t_{n+1}}\left(\int_{t-\tau}^{t}\widetilde{f}_{tt}(\cdot,s)\,ds\right)dt,v_h\right)\\
&\le\tau^2\|\widetilde{f}_{tt}\|_{L^\infty(0,T;L^2(\Omega))}\|v_h\|_0.
\end{aligned}\tag{5.12}$$

Using Lemma 3.1, we can get

$$Err_5 = \left(u_t^{n+1} - \frac{U^{n+1}}{2\tau}, v_h\right) \le C\tau^2 \|u_{ttt}\|_{L^\infty(0,T;L^2(\Omega))}\|v_h\|_0. \tag{5.13}$$

By the property of the projection operator, we have

$$Err_6 = \left(\frac{U^{n+1} - P^h U^{n+1}}{2\tau}, v_h\right) \le Ch^{k+1}\tau^{-1}\|U^{n+1}\|_{H^{k+1}(\Omega)}\|v_h\|_0 \le Ch^{k+1}\|u_t\|_{L^\infty(0,T;H^{k+1}(\Omega))}\|v_h\|_0. \tag{5.14}$$

Err_7 can be approximated via the stability of the bilinear form, the property of the projection operator, and (5.14),

$$\begin{aligned} Err_7 = m_h\left(\frac{\Pi_K^0 U^{n+1} - P^h U^{n+1}}{2\tau}, v_h\right) &\le \frac{\beta^*}{2\tau}(\|\Pi_K^0 U^{n+1} - U^{n+1}\|_0 + \|U^{n+1} - P^h U^{n+1}\|_0)\|v_h\|_0 \\ \le \frac{\beta^*}{2\tau} Ch^{k+1}\|U^{n+1}\|_{H^{k+1}(\Omega)}\|v_h\|_0 &\le Ch^{k+1}\|u_t\|_{L^\infty(0,T;H^{k+1}(\Omega))}\|v_h\|_0. \end{aligned} \tag{5.15}$$

Combining (5.9)–(5.15), we have

$$m_h\left(\frac{3A^{n+1} - 4A^n + A^{n-1}}{2\tau}, v_h\right) + \varepsilon a_h(A^{n+1}, v_h) \le \mathcal{R}_{h,\tau}\|v_h\|_0 + L\|A^{n+1}\|_0\|v_h\|_0. \tag{5.16}$$

Setting $v_h = A^{n+1}$ in (5.16) and $a_h(A^{n+1}, A^{n+1}) \ge 0$, we have

$$m_h(\frac{3A^{n+1} - 4A^n + A^{n-1}}{2\tau}, A^{n+1}) \le \mathcal{R}_{h,\tau}\|A^{n+1}\|_0 + L\|A^{n+1}\|_0^2. \tag{5.17}$$

By simple computation, we obtain

$$\begin{aligned} m_h\left(\frac{3A^{n+1} - 4A^n + A^{n-1}}{2\tau}, A^{n+1}\right) =& \frac{1}{4\tau}(\left\|A^{n+1}\right\|_{m_h}^2 - \|A^n\|_{m_h}^2 + \left\|2A^{n+1} - A^n\right\|_{m_h}^2 \\ &- \left\|2A^n - A^{n-1}\right\|_{m_h}^2 + \left\|A^{n+1} - 2A^n + A^{n-1}\right\|_{m_h}^2). \end{aligned} \tag{5.18}$$

Further, $\forall\ 0 < s < 1$, and we have

$$\begin{aligned} \left\|A^{n+1} - 2A^n + A^{n-1}\right\|_{m_h}^2 &= \left\|A^{n+1} - (2A^n - A^{n-1})\right\|_{m_h}^2 \\ &= \left\|A^{n+1}\right\|_{m_h}^2 + \left\|2A^n - A^{n-1}\right\|_{m_h}^2 - 2m_h(A^{n+1}, 2A^n - A^{n-1}) \\ &\ge \left\|A^{n+1}\right\|_{m_h}^2 + \left\|2A^n - A^{n-1}\right\|_{m_h}^2 - (s\left\|A^{n+1}\right\|_{m_h}^2 + \frac{1}{s}\left\|2A^n - A^{n-1}\right\|_{m_h}^2) \\ &= (1-s)\left\|A^{n+1}\right\|_{m_h}^2 + (1 - \frac{1}{s})\left\|2A^n - A^{n-1}\right\|_{m_h}^2. \end{aligned} \tag{5.19}$$

Substituting (5.19) into (5.18) yields

$$\begin{aligned} m_h\left(\frac{3A^{n+1} - 4A^n + A^{n-1}}{2\tau}, A^{n+1}\right) \ge& \frac{1}{4\tau}((2-s)\left\|A^{n+1}\right\|_{m_h}^2 - \|A^n\|_{m_h}^2 \\ &+ \left\|2A^{n+1} - A^n\right\|_{m_h}^2 - \frac{1}{s}\left\|2A^n - A^{n-1}\right\|_{m_h}^2), \end{aligned} \tag{5.20}$$

which together with (4.3), (5.17), and multiplying both sides by 4τ yields

$$\begin{aligned}
&(2-s)\left\|A^{n+1}\right\|_{m_h}^2 - \|A^n\|_{m_h}^2 + \left\|2A^{n+1}-A^n\right\|_{m_h}^2 - \frac{1}{s}\left\|2A^n - A^{n-1}\right\|_{m_h}^2 \\
&\le \tau\mathcal{R}_{h,\tau}\|A^{n+1}\|_0 + 4L\tau\|A^{n+1}\|_0^2 \le (\tau\mathcal{R}_{h,\tau}^2 + \tau\|A^{n+1}\|_0^2) + 4L\tau\|A^{n+1}\|_0^2 \\
&\le \tau\mathcal{R}_{h,\tau}^2 + (1+4L)\tau\|A^{n+1}\|_0^2 \le \tau\mathcal{R}_{h,\tau}^2 + \frac{1+4L}{\beta_*}\tau\left\|A^{n+1}\right\|_{m_h}^2 \\
&\triangleq \tau\mathcal{R}_{h,\tau}^2 + \bar{c}_0\tau\left\|A^{n+1}\right\|_{m_h}^2,
\end{aligned} \tag{5.21}$$

where $\bar{c}_0 = \frac{1+4L}{\beta_*}$. Subsequently, rearranging the terms yields

$$(2-s-\bar{c}_0\tau)\left\|A^{n+1}\right\|_{m_h}^2 - \|A^n\|_{m_h}^2 + \left\|2A^{n+1}-A^n\right\|_{m_h}^2 - \frac{1}{s}\left\|2A^n - A^{n-1}\right\|_{m_h}^2 \le \tau\mathcal{R}_{h,\tau}^2. \tag{5.22}$$

Setting $s = 1 - \frac{\bar{c}_0}{2}\tau \triangleq 1 - c_0\tau, c_0 = \frac{\bar{c}_0}{2}$, for sufficiently small τ, we have $0 < s < 1$, and substituting it into Eq (5.22), we obtain the following recurrence relation

$$s\left\|A^{n+1}\right\|_{m_h}^2 + \left\|2A^{n+1}-A^n\right\|_{m_h}^2 - \frac{1}{s^{n-1}}\left\|A^1\right\|_{m_h}^2 - \frac{1}{s^n}\left\|2A^1 - A^0\right\|_{m_h}^2 \le (1+\frac{1}{s}+\cdots+\frac{1}{s^{n-1}})\tau\mathcal{R}_{h,\tau}^2. \tag{5.23}$$

Omitting

$$\left\|2A^{n+1}-A^n\right\|_{m_h}^2 \ge 0,$$

and dividing both sides by s, we obtain

$$\left\|A^{n+1}\right\|_{m_h}^2 \le \frac{1}{s^n}\left\|A^1\right\|_{m_h}^2 + \frac{1}{s^{n+1}}\left\|2A^1 - A^0\right\|_{m_h}^2 + \frac{1}{s}(1+\frac{1}{s}+\cdots+\frac{1}{s^{n-1}})\tau\mathcal{R}_{h,\tau}^2. \tag{5.24}$$

Let $m = \frac{N-c_0T}{c_0T}$, and we get

$$\frac{N}{m} = \frac{c_0TN}{N-c_0T} = \frac{c_0T}{1-\frac{c_0T}{N}} \le 2c_0T,$$

then with a simple computation, we have

$$\frac{1}{s^n} < \frac{1}{s^{n+1}} = (\frac{1}{1-c_0\tau})^{n+1} = (1+\frac{1}{m})^{n+1} \le (\lim_{m_0\to\infty}(1+\frac{1}{m_0})^{m_0})^{\frac{N}{m}} = e^{\frac{N}{m}} \le e^{2c_0T}. \tag{5.25}$$

By using (5.25) and $0 < s < 1$, we obtain

$$\frac{1}{s}(1+\frac{1}{s}+\cdots+\frac{1}{s^{n-1}}) = \frac{1}{s^n}(\frac{1-s^n}{1-s}) = \frac{1}{s^n}\cdot\frac{1-s^n}{c_0}\cdot\frac{1}{\tau} \le (\frac{1}{c_0}e^{2c_0T})\frac{1}{\tau}. \tag{5.26}$$

Then, substituting (5.25) and (5.26) into (5.24) yields

$$\left\|A^{n+1}\right\|_{m_h} \le C(\left\|A^1\right\|_{m_h} + \left\|A^0\right\|_{m_h} + \mathcal{R}_{h,\tau}).$$

Using the second equation of (3.2), we obtain $A^0 = 0$, so

$$\left\|A^{n+1}\right\|_{m_h} \le C(\left\|A^1\right\|_{m_h} + \mathcal{R}_{h,\tau}). \tag{5.27}$$

Furthermore, from the equivalence between the $m_h(\cdot,\cdot)$ norm and the L^2 norm, we obtain

$$\|A^{n+1}\|_0 \le C(\|A^1\|_0 + \mathcal{R}_{h,\tau}) \le C(\|u_h^1 - u^1\|_0 + \mathcal{R}_{h,\tau}). \tag{5.28}$$

Combining (5.28) and (5.5), we complete the proof. □

Remark 5.1. *The first value u_h^1 is computed by the BDF1, which coincides with the backward Euler method in the present setting. We use the same step size as in the BDF2 scheme:*

$$\tau_1 = \tau.$$

The variational BDF1 initialization is to find $u_h^1 \in V_h$ such that

$$m_h\left(\frac{u_h^1 - u_h^0}{\tau_1}, v_h\right) + \varepsilon a_h(u_h^1, v_h) + (\widetilde{f_h}(u_h^0), v_h) = 0, \qquad \forall v_h \in V_h, \tag{5.29}$$

where $u_h^0 = P^h u^0$.

Although backward Euler is globally first-order when used repeatedly over a fixed time interval, a single backward Euler step has an $O(\tau^2)$ solution error under sufficient temporal regularity. Consequently,

$$\|u_h^1 - u^1\|_0 \le C(h^{k+1} + \tau^2) \tag{5.30}$$

and

$$|u_h^1 - u^1|_{1,h} \le C(h^k + \tau^2). \tag{5.31}$$

These estimates provide sufficiently accurate starting values for the subsequent BDF2 recurrence. Therefore, the single BDF1 initialization does not reduce the global second-order temporal convergence.

5.2. Error estimate in the H^1-seminorm

Lemma 5.1. *For every $v_h \in V_h$, define $\Delta_h v_h \in V_h$ by*

$$m_h(\Delta_h v_h, w_h) = -a_h(v_h, w_h), \qquad \forall w_h \in V_h. \tag{5.32}$$

Since V_h is finite-dimensional and $m_h(\cdot,\cdot)$ is symmetric and positive definite, $\Delta_h v_h$ exists uniquely. Thus, Δ_h: $V_h \to V_h$ is well-defined and computable.

Moreover, for all $v_h, w_h \in V_h$,

$$m_h(-\Delta_h v_h, w_h) = a_h(v_h, w_h), \tag{5.33}$$

$$m_h(\Delta_h v_h, w_h) = m_h(v_h, \Delta_h w_h) \tag{5.34}$$

and

$$m_h(-\Delta_h v_h, v_h) = a_h(v_h, v_h) \ge 0. \tag{5.35}$$

Finally,

$$a_h(v_h, -\Delta_h v_h) = m_h(\Delta_h v_h, \Delta_h v_h) \ge \beta_* \|\Delta_h v_h\|_0^2. \tag{5.36}$$

Theorem 5.2. *Let $u^{n+1} = u(\cdot, t_{n+1})$, and let u_h^{n+1} be the solution of* (3.2)*. Under the regularity assumptions* (5.1)*, there exists a constant $C_\varepsilon > 0$, independent of h and τ, such that*

$$|u_h^{n+1} - u^{n+1}|_{1,h} \le C_\varepsilon(h^k + \tau^2). \tag{5.37}$$

Proof. Since $a_h(\cdot,\cdot)$ is symmetric, through simple calculation, the following formula holds

$$\begin{aligned}2a_h(3A^{n+1}-4A^n+A^{n-1},A^{n+1}) = {} & a_h(A^{n+1},A^{n+1})-a_h(A^n,A^n)+a_h(2A^{n+1}-A^n,2A^{n+1}-A^n)\\ & -a_h(2A^n-A^{n-1},2A^n-A^{n-1})\\ & +a_h(A^{n+1}-2A^n+A^{n-1},A^{n+1}-2A^n+A^{n-1}),\end{aligned} \tag{5.38}$$

and from the nonnegativity of the last term, it follows that

$$\begin{aligned}2a_h(3A^{n+1}-4A^n+A^{n-1},A^{n+1}) \geq {} & a_h(A^{n+1},A^{n+1})-a_h(A^n,A^n)\\ & +a_h(2A^{n+1}-A^n,2A^{n+1}-A^n)\\ & -a_h(2A^n-A^{n-1},2A^n-A^{n-1}).\end{aligned} \tag{5.39}$$

Then, we rewrite (5.16) into a simplified form

$$m_h\left(\frac{3A^{n+1}-4A^n+A^{n-1}}{2\tau},v_h\right)+\varepsilon a_h(A^{n+1},v_h) \leq C(\mathcal{R}_{h,\tau}+\|A^{n+1}\|_0)\|v_h\|_0, \tag{5.40}$$

substituting the result for $\|A^{n+1}\|_0$ into (5.40) yields

$$m_h\left(\frac{3A^{n+1}-4A^n+A^{n-1}}{2\tau},v_h\right)+\varepsilon a_h(A^{n+1},v_h) \leq C\mathcal{R}_{h,\tau}\|v_h\|_0. \tag{5.41}$$

Next, the proof proceeds similarly to Theorem 5.1. Setting $v_h=-\Delta_h A^{n+1}$ in (5.41), we can get

$$\frac{1}{4\tau}\cdot 2m_h\left(3A^{n+1}-4A^n+A^{n-1},-\Delta_h A^{n+1}\right)+\varepsilon a_h(A^{n+1},-\Delta_h A^{n+1}) \leq C\mathcal{R}_{h,\tau}\|\Delta_h A^{n+1}\|_0. \tag{5.42}$$

By the definition of Δ_h in Lemma 5.1,

$$\begin{aligned}m_h(3A^{n+1}-4A^n+A^{n-1},-\Delta_h A^{n+1}) &= a_h(3A^{n+1}-4A^n+A^{n-1},A^{n+1}),\\ a_h(A^{n+1},-\Delta_h A^{n+1}) &= m_h(\Delta_h A^{n+1},\Delta_h A^{n+1}).\end{aligned} \tag{5.43}$$

Therefore, by (5.36) and (5.39), we obtain

$$\begin{aligned}&\frac{1}{4\tau}\cdot 2m_h\left(3A^{n+1}-4A^n+A^{n-1},-\Delta_h A^{n+1}\right)+\varepsilon a_h(A^{n+1},-\Delta_h A^{n+1})\\ &=\frac{1}{4\tau}\cdot 2a_h\left(3A^{n+1}-4A^n+A^{n-1},A^{n+1}\right)+\varepsilon m_h(\Delta_h A^{n+1},\Delta_h A^{n+1})\\ &\geq \frac{1}{4\tau}(a_h(A^{n+1},A^{n+1})-a_h(A^n,A^n)+a_h(2A^{n+1}-A^n,2A^{n+1}-A^n)\\ &\quad -a_h(2A^n-A^{n-1},2A^n-A^{n-1}))+\varepsilon\beta_*\|\Delta_h A^{n+1}\|_0^2.\end{aligned} \tag{5.44}$$

Young's inequality gives

$$C\mathcal{R}_{h,\tau}\|\Delta_h A^{n+1}\|_0 \leq \frac{(C\mathcal{R}_{h,\tau})^2}{4\varepsilon\beta_*}+\varepsilon\beta_*\|\Delta_h A^{n+1}\|_0^2. \tag{5.45}$$

Combining (5.42)–(5.45) yields

$$\begin{aligned} &a_h(A^{n+1}, A^{n+1}) - a_h(A^n, A^n) + a_h(2A^{n+1} - A^n, 2A^{n+1} - A^n) \\ &- a_h(2A^n - A^{n-1}, 2A^n - A^{n-1}) \le \frac{C\tau}{\varepsilon\beta_*}\mathcal{R}^2_{h,\tau}. \end{aligned} \tag{5.46}$$

Summing (5.46) from 1 to n and using $n\tau \le T$, we obtain

$$\begin{aligned} &a_h(A^{n+1}, A^{n+1}) - a_h(A^1, A^1) + a_h(2A^{n+1} - A^n, 2A^{n+1} - A^n) \\ &- a_h(2A^1 - A^0, 2A^1 - A^0) \le \frac{C}{\varepsilon\beta_*}\mathcal{R}^2_{h,\tau} \cdot (\tau n) \le \frac{C}{\varepsilon\beta_*}\mathcal{R}^2_{h,\tau}, \end{aligned} \tag{5.47}$$

which together with $a_h(2A^{n+1} - A^n, 2A^{n+1} - A^n) \ge 0$, it is easy to obtain

$$a_h(A^{n+1}, A^{n+1}) \le C(a_h(A^1, A^1) + a_h(A^0, A^0)) + \frac{C}{\varepsilon\beta_*}\mathcal{R}^2_{h,\tau} \le Ca_h(A^1, A^1) + \frac{C}{\varepsilon\beta_*}\mathcal{R}^2_{h,\tau}, \tag{5.48}$$

where $A^0 = u_h^0 - P^h u^0 = 0$ is used. Equation (5.48) and the stability of $a_h(\cdot,\cdot)$ yield

$$|A^{n+1}|^2_{1,h} \le \frac{1}{\alpha_*}a_h(A^{n+1}, A^{n+1}) \le C|A^1|^2_{1,h} + \frac{C}{\varepsilon\beta_*}\mathcal{R}^2_{h,\tau}. \tag{5.49}$$

Applying (2.1) in Lemma 2.1 and (5.31) in Remark 5.1, we have the estimate of $|A^1|_{1,h}$ as follows

$$|A^1|_{1,h} = |u_h^1 - P^h u^1|_{1,h} = |u_h^1 - u^1 + (u^1 - P^h u^1)|_{1,h} \le |u_h^1 - u^1|_{1,h} + |u^1 - P^h u^1|_{1,h} \le C(h^k + \tau^2). \tag{5.50}$$

Substituting (5.50) into (5.49) yields

$$|A^{n+1}|_{1,h} \le C_\varepsilon(h^k + \tau^2). \tag{5.51}$$

Thus, we have

$$|u_h^{n+1} - u^n|_{1,h} \le |A^{n+1}|_{1,h} + |B^{n+1}|_{1,h} \le C_\varepsilon(h^k + \tau^2), \tag{5.52}$$

which completes the proof of the Theorem 5.2. □

6. Numerical experiments

6.1. Convergence test with a manufactured solution

In this subsection, we verify the theoretical convergence rates. We take

$$\Omega = (0,1)^2, \qquad T = 1, \qquad \varepsilon = 1,$$

and use the lowest-order nonconforming virtual element space, namely, $k = 1$.

We consider

$$\begin{cases} u_t = \varepsilon(u_{xx} + u_{yy}) - \widetilde{f}(u) + h(x,y,t), & (x,y) \in \Omega, \\ u(x,y,0) = x^3(1-x)^3y^3(1-y)^3, \\ u(0,y,t) = u(1,y,t) = 0, \\ u(x,0,t) = u(x,1,t) = 0. \end{cases} \tag{6.1}$$

The exact solution is

$$u(x, y, t) = e^{-t} x^3 (1 - x)^3 y^3 (1 - y)^3.$$

We take

$$M = 1.$$

Since this exact solution satisfies

$$|u(x, y, t)| < 1 \quad \text{on} \quad \overline{\Omega} \times [0, T],$$

the truncated nonlinear function $\widetilde{f}(u)$ coincides with the original cubic nonlinear function $u^3 - u$. Therefore, the truncation does not alter the exact solution or the convergence results in this experiment.

The forcing term is

$$\begin{aligned} h(x, y, t) = {} & e^{-t} x^3 (1 - x)^3 y^3 (1 - y)^3 \left[e^{-2t} x^6 (1 - x)^6 y^6 (1 - y)^6 - 2 \right] \\ & - e^{-t} y^3 (1 - y)^3 \left[6x(1 - x)^3 - 18x^2 (1 - x)^2 + 6x^3 (1 - x) \right] \\ & - e^{-t} x^3 (1 - x)^3 \left[6y(1 - y)^3 - 18y^2 (1 - y)^2 + 6y^3 (1 - y) \right]. \end{aligned} \tag{6.2}$$

Tables 1 and 2 show the spatial and temporal convergence results, respectively. More clearly, the results are also plotted in Figures 1 and 2. The numerical results confirm the theoretical convergence rates.

Table 1. Spatial convergence results.

h	$\|u_h^{n+1} - u^{n+1}\|_0$	Order	$\|u_h^{n+1} - u^{n+1}\|_{1,h}$	Order
0.1250	1.3605e-06	–	4.9450e-05	–
0.0625	2.8261e-07	2.2673	2.4586e-05	1.0081
0.0313	6.7035e-08	2.0758	1.2282e-05	1.0013
0.0156	1.7815e-08	1.9119	6.1403e-06	1.0002

Table 2. Temporal convergence results.

τ	$\|u_h^{n+1} - u^{n+1}\|_0$	Order	$\|u_h^{n+1} - u^{n+1}\|_{1,h}$	Order
0.0833	5.2937e-07	–	4.3446e-05	–
0.0417	1.2059e-07	2.1341	1.2924e-05	1.7492
0.0208	3.0218e-08	1.9967	3.2595e-06	1.9873
0.0104	9.2037e-09	1.7151	7.6730e-07	2.0868

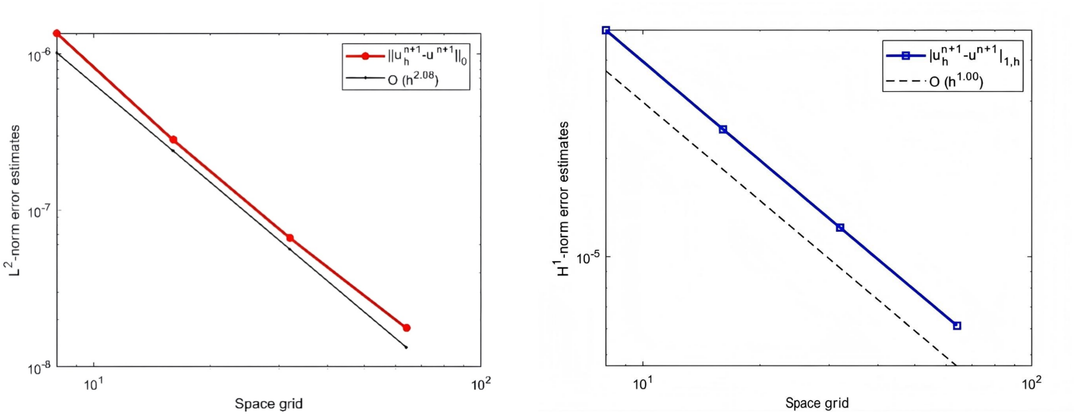

Figure 1. The L^2-norm error (left) and the H^1-seminorm error (right) for the spatial convergence test with $\tau = 1/64$.

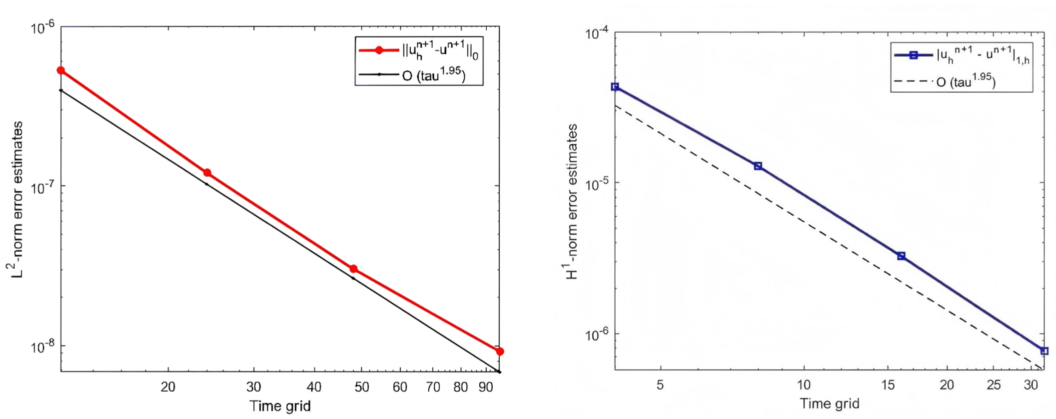

Figure 2. The L^2-norm error (left) and the H^1-seminorm error (right) for the temporal convergence test with $h = 1/64$.

6.2. *Shrinking circular-interface benchmark*

The manufactured-solution test verifies the convergence orders, but the artificial forcing term masks the gradient-flow character of the Allen-Cahn equation. We therefore consider a standard source-free shrinking circular-interface benchmark:

$$\begin{cases} u_t - \varepsilon\Delta u + \widetilde{f}(u) = 0, & (x,y,t) \in \Omega \times (0,T], \\ u = u_0, & (x,y,t) \in \partial\Omega \times (0,T], \\ u(x,y,0) = u_0(x,y), & (x,y) \in \Omega. \end{cases} \tag{6.3}$$

Here $\Omega = (0,1)^2$, and the initial value is the circular diffuse profile

$$u_0(x,y) = \tanh\left(\frac{R_0 - \sqrt{(x-x_c)^2 + (y-y_c)^2}}{\sqrt{2\varepsilon}}\right). \tag{6.4}$$

For the truncated potential we take $M = 1$, and we set

$$\varepsilon = 5 \times 10^{-3}, \quad (x_c, y_c) = (0.5, 0.5), \quad R_0 = 0.25, \quad T = 10.$$

The trace of Eq (6.4), which is already close to -1 on $\partial\Omega$, is held fixed during the evolution, so the boundary does not inject energy. The quadratic nonconforming virtual element space is used on a 16×16 polygonal mesh.

We employ BDF2 with the fixed time-step size

$$\tau = 5 \times 10^{-3}.$$

Thus, the computation reaches $T = 10$ in 2000 time steps.

During the computation, we monitor the discrete physical energy

$$E_h(u_h^n) = \frac{\varepsilon}{2} a_h(u_h^n, u_h^n) + \sum_{K \in \mathcal{T}_h} \int_K \widetilde{F}(\Pi_K^0 u_h^n)\, dx$$

and the equivalent radius

$$R_h^n = \sqrt{\frac{|\{(x, y) \in \Omega : \Pi_h^0 u_h^n(x, y) \geq 0\}|}{\pi}}. \tag{6.5}$$

The computed phase was numerically observed to remain in $[-1, 1]$, so the truncated and quartic double-well potentials coincide in this experiment.

Figure 3 shows the expected curvature-driven shrinkage and eventual disappearance of the positive phase. The equivalent radius decreases from $R_h^0 = 0.250316$ to $R_h^N = 0$. Figure 4 shows that the discrete energy decreases from $E_h(u_h^0) = 1.047135363883 \times 10^{-1}$ to $E_h(u_h^N) = 1.071191118684 \times 10^{-5}$. The largest energy increment over all 2000 steps is -2.115×10^{-9}; hence

$$E_h(u_h^{n+1}) \leq E_h(u_h^n)$$

at every accepted time level. The experiment therefore demonstrates both curvature-driven interface motion and energy dissipation without an artificial source term.

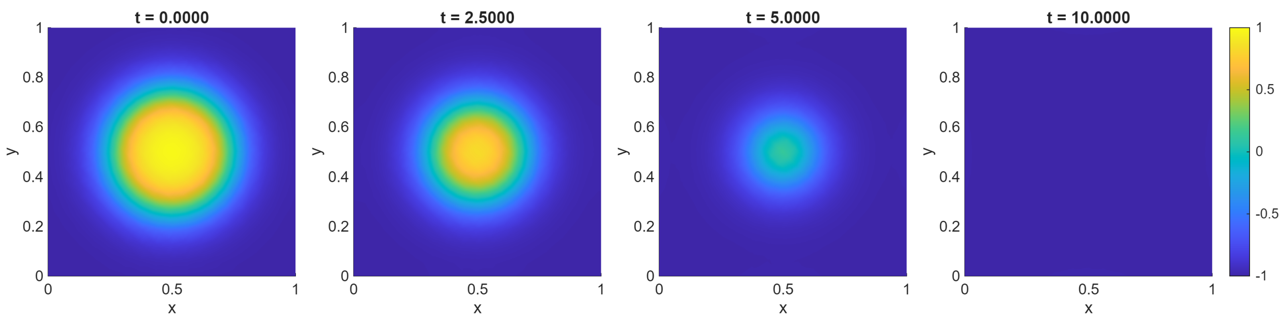

Figure 3. Evolution of the circular diffuse interface at $t = 0$, 2.5, 5, and 10. The positive phase enclosed by the zero level set shrinks and eventually disappears.

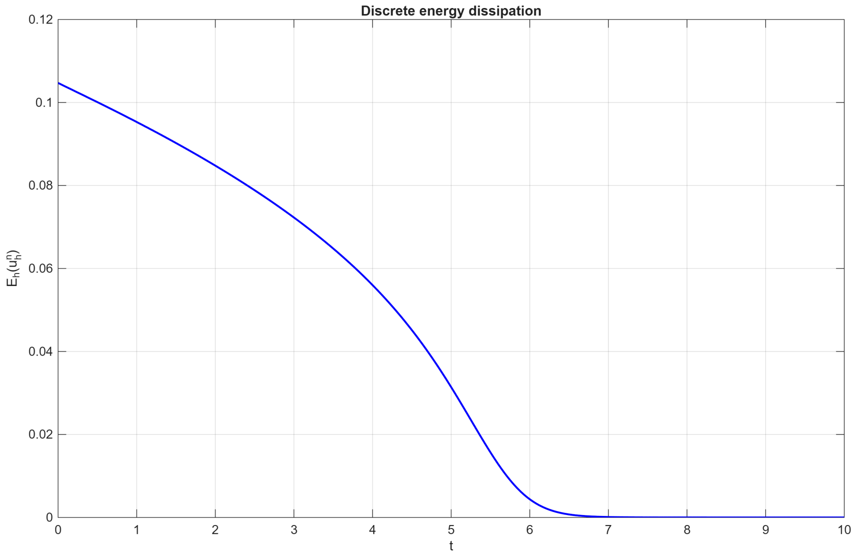

Figure 4. Evolution of the physical energy $E_h(u_h^n)$.

7. Conclusions

In this paper, we developed an IMEX BDF2 nonconforming virtual element scheme for the Allen-Cahn equation on polygonal meshes. An explicitly defined truncated polynomial potential of Shen and Yang [2] was employed to rigorously guarantee the global Lipschitz continuity of the nonlinear term. The truncated potential coincides with the standard quartic double-well potential on $[-M, M]$ and has quadratic growth outside this interval.

Under a suitable time-step restriction, the proposed method satisfies a modified discrete energy dissipation law. By combining the nonconforming energy projection with a discrete Laplace operator adapted to the virtual element space, we established optimal convergence rates of order $O(h^{k+1} + \tau^2)$ in the L^2-norm and $O(h^k + \tau^2)$ in the H^1-seminorm. The manufactured-solution experiment confirms the theoretical spatial and temporal convergence rates. In addition, the source-free shrinking circular-interface benchmark exhibits curvature-driven interface motion and monotone decay of the discrete physical energy.

Future work will focus on two aspects: (i) adaptive mesh refinement with variable-step BDF2 stability and error analysis; (ii) extensions to broader gradient-flow systems, including multi-phase and elasticity-coupled phase-field models, together with maximum-principle-preserving discretizations and fast solvers.

Author contributions

Peizhen Wang: conceptualization, methodology, numerical scheme design, theoretical analysis, writing-original draft preparation, writing-review and editing, final approval; Wang Liu: numerical scheme development, theoretical analysis, numerical experiments, writing-review and editing; Jinyang Xia: theoretical verification, assistance in numerical experiments, literature review, writing-initial draft preparation. All authors have read and approved the final version of the manuscript for publication.

Use of Generative-AI tools declaration

The authors declare they have not used Artificial Intelligence (AI) tools in the creation of this article.

Acknowledgments

This work was supported by the National Natural Science Foundation of China (Grant No. 11901197) and the Young Teacher Foundation of Henan Province (Grant No. 2021GGJS080).

Conflict of interest

The authors declare that there are no conflicts of interest.

References

1. S. M. Allen, J. W. Cahn, A microscopic theory for antiphase boundary motion and its application to antiphase domain coarsening, *Acta Metall.*, **27** (1979), 1085–1095. https://doi.org/10.1016/0001-6160(79)90196-2
2. J. Shen, X. Yang, Numerical approximations of Allen-Cahn and Cahn-Hilliard equations, *Discrete Contin. Dyn. Syst.*, **28** (2010), 1669–1691. https://doi.org/10.3934/dcds.2010.28.1669
3. S. Orizaga, G. G. Parra, L. Forman, J. Villegas-Villanueva, Solving Allen-Cahn equations with periodic and nonperiodic boundary conditions using mimetic finite-difference operators, *Appl. Math. Comput.*, **484** (2025), 128993. https://doi.org/10.1016/j.amc.2024.128993
4. C. Lee, Y. Choi, J. Kim, An explicit stable finite difference method for the Allen-Cahn equation, *Appl. Numer. Math.*, **182** (2022), 87–99. https://doi.org/10.1016/j.apnum.2022.08.006
5. Z. Q. Tan, C. J. Zhang, The discrete maximum principle and energy stability of a new second-order difference scheme for Allen-Cahn equations, *Appl. Numer. Math.*, **166** (2021), 227–237. https://doi.org/10.1016/j.apnum.2021.04.010
6. Q. Du, L. L. Ju, X. Li, Z. H. Qiao, Maximum principle preserving exponential time differencing schemes for the nonlocal Allen-Cahn equation, *SIAM J. Numer. Anal.*, **57** (2019), 875–898. https://doi.org/10.1137/18M118236X
7. P. Manorot, B. Wongsaijai, K. Poochinapan, Performance of a new stabilized structure-preserving finite element method for the Allen-Cahn equation, *Math. Comput. Model. Dyn. Syst.*, **30** (2024), 972–1008. https://doi.org/10.1080/13873954.2024.2421835
8. J. Yang, N. Y. Yi, H. Zhang, High-order unconditionally maximum-principle preserving finite element method for the Allen-Cahn equation, *Appl. Numer. Math.*, **188** (2023), 42–61. https://doi.org/10.1016/j.apnum.2023.03.002
9. G. Akrivis, B. Li, Error estimates for fully discrete BDF finite element approximations of the Allen-Cahn equation, *IMA J. Numer. Anal.*, **42** (2022), 363–391. https://doi.org/10.1093/imanum/draa065

10. Y. Liu, X. Q. Shen, Z. Guan, Y. F. Nie, The adaptive SAV weak Galerkin finite element method for the Allen-Cahn equation, *Comput. Math. Appl.*, **151** (2023), 449–460. https://doi.org/10.1016/j.camwa.2023.10.023

11. X. P. Wang, F. Z. Gao, J. T. Cui, Z. J. Sun, A weak Galerkin finite element method for the Allen-Cahn equation with a nonuniform two-step backward differentiation formula scheme, *Numer. Methods Partial Differ. Equations*, **39** (2023), 2227–2243. https://doi.org/10.1002/num.22964

12. R. Li, Y. L. Gao, Z. X. Chen, Adaptive discontinuous Galerkin finite element methods for the Allen-Cahn equation on polygonal meshes, *Numer. Algorithms*, **95** (2024), 1981–2014. https://doi.org/10.1007/s11075-023-01635-5

13. L. B. da Veiga, F. Brezzi, A. Cangiani, G. Manzini, L. D. Marini, A. Russo, Basic principles of virtual element methods, *Math. Models Methods Appl. Sci.*, **23** (2013), 199–214. https://doi.org/10.1142/S0218202512500492

14. G. Vacca, L. B. da Veiga, Virtual element methods for parabolic problems on polygonal meshes, *Numer. Methods Partial Differ. Equations*, **31** (2015), 2110–2134. https://doi.org/10.1002/num.21982

15. B. J. Zhang, M. F. Feng, Virtual element method for two-dimensional linear elasticity problems in a mixed weakly symmetric formulation, *Appl. Math. Comput.*, **328** (2018), 1–25. https://doi.org/10.1016/j.amc.2018.01.023

16. L. B. da Veiga, F. Dassi, G. Vacca, The Stokes complex for virtual elements in three dimensions, *Math. Models Methods Appl. Sci.*, **30** (2020), 477–512. https://doi.org/10.1142/S0218202520500128

17. L. B. da Veiga, F. Dassi, G. Manzini, L. Mascotto, Virtual elements for Maxwell's equations, *Comput. Math. Appl.*, **116** (2022), 82–99. https://doi.org/10.1016/j.camwa.2021.08.019

18. Y. P. Chen, Q. L. Gu, J. Huang, Step-by-step solving virtual element schemes based on the scalar auxiliary variable approach with relaxation for Allen-Cahn-type gradient flows, *Math. Models Methods Appl. Sci.*, **34** (2024), 2141–2167. https://doi.org/10.1142/S0218202524500453

19. P. F. Antonietti, L. B. da Veiga, S. Scacchi, M. Verani, A C^1 virtual element method for the Cahn-Hilliard equation with polygonal meshes, *SIAM J. Numer. Anal.*, **54** (2016), 34–56. https://doi.org/10.1137/15M1008117

20. B. A. de Dios, K. Lipnikov, G. Manzini, The nonconforming virtual element method, *ESAIM Math. Model. Numer. Anal.*, **50** (2016), 879–904. https://doi.org/10.1051/m2an/2015090

21. A. Cangiani, V. Gyrya, G. Manzini, The nonconforming virtual element method for the Stokes equations, *SIAM J. Numer. Anal.*, **54** (2016), 3411–3435. https://doi.org/10.1137/15M1049531

22. X. Liu, Z. X. Chen, The nonconforming virtual element method for the Navier-Stokes equations, *Adv. Comput. Math.*, **45** (2019), 51–74. https://doi.org/10.1007/s10444-018-9602-z

23. B. Zhang, J. K. Zhao, M. Li, The divergence-free nonconforming virtual element method for the Navier-Stokes problem, *Numer. Methods Partial Differ. Equations*, **39** (2023), 1977–1995. https://doi.org/10.1002/num.22812

24. J. K. Zhao, B. Zhang, S. P. Mao, S. C. Chen, The nonconforming virtual element method for the Darcy-Stokes problem, *Comput. Methods Appl. Mech. Eng.*, **370** (2020), 113251. https://doi.org/10.1016/j.cma.2020.113251
25. M. Li, L. L. Wang, N. Wang, Variable-time-step BDF2 nonconforming VEM for coupled Ginzburg-Landau equations, *Appl. Numer. Math.*, **186** (2023), 378–410. https://doi.org/10.1016/j.apnum.2023.01.022
26. J. K. Zhao, S. C. Chen, B. Zhang, The nonconforming virtual element method for plate-bending problems, *Math. Models Methods Appl. Sci.*, **26** (2016), 1671–1687. https://doi.org/10.1142/S021820251650041X
27. J. K. Zhao, T. L. Wang, B. Zhang, The stabilized nonconforming virtual element method for linear elasticity problems, *J. Sci. Comput.*, **92** (2022), 31. https://doi.org/10.1007/s10915-022-01927-3
28. A. Dedner, A. Hodson, A higher-order nonconforming virtual element method for the Cahn-Hilliard equation, *J. Sci. Comput.*, **101** (2024), 81. https://doi.org/10.1007/s10915-024-02721-z
29. B. A. de Dios, K. Lipnikov, G. Manzini, The nonconforming virtual element method, *ESAIM Math. Model. Numer. Anal.*, **50** (2016), 879–904. https://doi.org/10.1051/m2an/2015090
30. J. K. Zhao, B. Zhang, X. P. Zhu, The nonconforming virtual element method for parabolic problems, *Appl. Numer. Math.*, **143** (2019), 97–111. https://doi.org/10.1016/j.apnum.2019.04.002
31. X. L. Feng, H. L. Song, T. Tang, J. Yang, Nonlinear stability of the implicit–explicit methods for the Allen-Cahn equation, *Inverse Probl. Imaging*, **7** (2013), 679–695. https://doi.org/10.3934/ipi.2013.7.679
32. D. Adak, E. Natarajan, S. Kumar, Convergence analysis of virtual element methods for semilinear parabolic problems on polygonal meshes, *Numer. Methods Partial Differ. Equations*, **35** (2019), 222–245. https://doi.org/10.1002/num.22298